Available online at www.sciencedirect.com
ScienceDirect
Journal of Photochemistry and Photobiology A: Chemistry 187 (2007) 348–355
Journal of Photochemistry and Photobiology A:Chemistry
www.elsevier.com/locate/jphotochem

An investigation of the photosubstitution reaction between N719-dyed nanocrystalline TiO_2 particles and 4-*tert*-butylpyridine

Farahnaz Nour-Mohammadi [a], Hoang Thai Nguyen [a], Gerrit Boschloo [b], Torben Lund [a,*]

[a] *Department of Life Sciences and Chemistry, Roskilde University, DK-4000 Roskilde, Denmark*
[b] *Department of Chemistry, Royal Institute of Technology, SE-10044 Stockholm, Sweden*

Received 30 June 2006; received in revised form 2 November 2006; accepted 5 November 2006
Available online 9 November 2006

Abstract

The effect of high concentrations of the solar cell additive 4-*tert*-butylpyridine (**4-TBP**) on the stability and lifetime of the sensitizer $[Ru(Hdcbpy)_2(NCS)_2]^{2-}$, $2(n\text{-}C_4H_9)_4N^+$, (H_2dcbpy = 2,2′-bipyridine-4,4′-dicarboxylic acid), known as **N719**, has been evaluated based on kinetic data obtained from simple model experiments. In these experiments, colloidal solutions of **N719**-dyed nanocrystalline TiO_2 particles in acetonitrile were irradiated with 532-nm laser light in the presence of 0–1 mol/l of **4-TBP**. Five degradation products were identified using LC–ESI-MS: the 4-*tert*-butylpyridine substitution product $[Ru(H_2dcbpy)(Hdcbpy)(NCS)(4\text{-}TBP)]$ (**SP**) and the products $[Ru(H_2dcbpy)_2(NCS)(CN)]$, $[Ru(H_2dcbpy)(Hdcbpy)(NCS)(CH_3CN)]$, $[Ru(H_2dcbpy)(Hdcbpy)(NCS)(H_2O)]$ and $[Ru(H_2dcbpy)_2(CN)_2]$ (**3–6**). The sum of the quantum yields of the five products, $\Phi_{deg} = (1.3 \pm 0.2) \times 10^{-4}$, was found to be independent of **4-TBP** concentration. Based on this observation, a degradation mechanism was proposed, in which the reaction proceeds through the rate-determining formation of a common intermediate complex, $I = [Ru^{II}(H_2dcbpy)_2(NCS)(NCS\cdot)]^+$. An average degradation rate of $k_{deg} = 6 \times 10^{-3}\ s^{-1}$ was obtained from the value of Φ_{deg} and the back electron-transfer rate, k_{back} of the reaction $TiO_2 + e^- \,|\, N719^+ \rightarrow TiO_2 \,|\, N719$, obtained by means of photo-induced absorption (PIA) measurements. The lifetime of the solar cell sensitizer **N719** was estimated to be between 34 years, based on k_{deg} and an average literature value of the regeneration rate, $k_{reg} = 2 \times 10^6\ M^{-1}\ s^{-1}$, of the reaction between $TiO_2 \,|\, N719^+$ and iodide. We conclude that the addition of **4-TBP** to dye-sensitized solar cells (DSSC) does not decrease the lifetime of the **N719** dye during normal solar cell operation at room temperature.

Keywords: N719; *tert*-Butylpyridine; Dye-sensitized solar cells; Stability; LC–ESI-MS

1. Introduction

Nanocrystalline dye-sensitized titanium dioxide solar cells (nc-DSSC) have attracted significant attention because of their good efficiency of solar-to-electric power conversion and lower cost compared to those of silicon solar cells [1–6]. The chemistry at the photo anode is described by Eqs. (1)–(3):

$$TiO_2|S \xrightarrow{h\nu} TiO_2|S^* \quad (1)$$

$$TiO_2|S^* \xrightarrow{k_{inj}} TiO_2 + e^-|S^+ \quad (2)$$

$$TiO_2|S^+ + red \xrightarrow{k_{reg}} TiO_2|S + ox \quad (3)$$

The sensitizer, S, is first excited by a photon; this is followed by an ultra-fast electron injection from S^* to the conduction band of the TiO_2 semiconductor. The cell cycle finishes after the regeneration of S by the reduced form of the mediator, which in most cases is iodide. One of the most popular sensitizers is the ruthenium dye known as **N719**, i.e., $[Ru(Hdcbpy)_2(NCS)_2]^{2-}$, $2(n\text{-}C_4H_9)_4N^+$, (H_2bdcbpy = L = 2,2′-bipyridine-4,4′-dicarboxylic acid), due to its high efficiency and stability [1–4]. The molecular structure is depicted in Fig. 1.

Various additives have been introduced into the cell electrolyte to improve cell performance [7–13]. One of the most commonly used additives is 4-*tert*-butylpyridine **(4-TBP),** as it has been shown to increase the open circuit voltage, V_{oc}, of the cell by 80–100 mV. It does this by suppressing the dark current arising from the recombination of electrons in the conduction band with the oxidized form of the mediator (I_3^-) [14,15].

* Corresponding author. Tel.: +45 46742472; fax: +45 46743011.
E-mail address: tlund@ruc.dk (T. Lund).

1010-6030/$ – see front matter © 2006 Elsevier B.V. All rights reserved.
doi:10.1016/j.jphotochem.2006.11.001

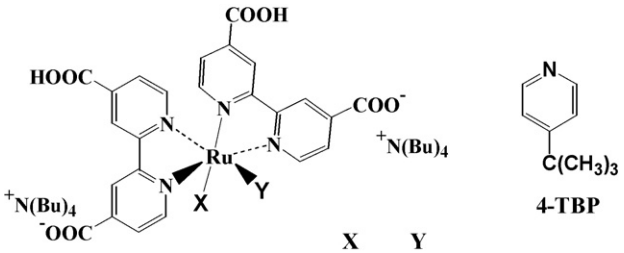

	X	Y
N719	NCS	NCS
2	SCN	NCS
SP	NCS	4-TBP
3	NCS	CH_3CN
4	NCS	CN
5	NCS	H_2O
6	CN	CN

Fig. 1. Molecular structures of the starting dye **N719** (including its minor isomer **2**) and the observed photolysis products **SP** and **3–6**.

Recently we found the substitution product, **SP**, i.e., Bu_4N^+, $[Ru(Hdcbpy)_2(NCS)(4\text{-TBP})]^-$ (see Fig. 1), in dye extracts from light-exposed nc-DSSC using **N719** as the sensitizer [16]. To the best of our knowledge, there have been no previous reports of possible side reactions of **N719** with 4-*tert*-butylpyridine in solar cells. The observation prompted us to investigate the kinetics of the substitution reaction, to be able to evaluate the influence of this reaction on the long-term stability of nc-DSSC.

The 4-*tert*-butylpyridine may react with the sensitizer in all its three states, i.e., S, S^*, and S^+. The substitution product, however, was mainly found in solar cells that had been exposed to light at room temperature [16]. Furthermore preliminary results from our laboratory show that **N719** does not react thermally with **4-TBP** in acetonitrile at room temperature. These observations indicate that at room temperature, the substitution product, **SP**, is mainly formed through the dye states S^* or S^+. The injection rate of S^* into the conduction band of the TiO_2 semiconductor is extremely fast ($k_{inj} = 10^{13}\ s^{-1}$) [17], and the pyridine additive therefore does not have enough time to react with S^*. Thus, it is most likely that the substitution reaction is initiated from the oxidized state of the sensitizer S^+ (Eq. (4)):

$$TiO_2|S^+ + \text{4-TBP} \xrightarrow{k_4} TiO_2|SP \quad (4)$$

$$TiO_2|S^+ \xrightarrow{k_5} TiO_2|DP \quad (5)$$

$$TiO_2 + e^-|S^+ \xrightarrow{k_{back}} TiO_2|S \quad (6)$$

Besides the substitution reaction Eq. (4) S^+ may undergo intramolecular and solvent dependant degradation reactions Eq. (5). In the case of S = **N719** these products lead to the degradation products **3–6** [18,21].

In this work, we have measured the quantum yield of the substitution product, Φ_{SP}, and the quantum yield of the sum of the degradation products **3–6**, Φ_{DP}, through model experiments similar to those by which we obtained the oxidative degradation reaction rate, k_5 [18]. The quantum yield experiments were performed by irradiating colloidal solutions of **N719**-dyed nanocrystalline TiO_2 particles in acetonitrile in the presence of high concentrations of 4-*tert*-butylpyridine. The chemistry of the model experiments is described by Eqs. (1), (2), and (4)–(6).

The work investigates the mechanism of the photo-initiated substitution reaction and evaluates the effect of 4-*tert*-butylpyridine on the overall $TiO_2 | S^+$ degradation rate, k_{deg}, with **N719** being used as the sensitizer. Based on the k_{deg} value, we have estimated the intrinsic lifetime of **N719** in light-exposed solar cells.

2. Experimental

2.1. Chemicals

The bis(tetrabutylammonium) salt of the complex *cis*-bis(isothiocyanato) bis(2,2′-bipyridyl-4,4′-dicarboxylato) ruthenium (II), with the trade name ruthenium 535-bis TBA and referred to as **N719**, was obtained from Solaronix SA (Aubonne, Switzerland). The *N*,*N*-dimethylformamide (DMF) and acetonitrile (ACN) used were of HPLC grade and were obtained from Merck. The 4-*tert*-butylpyridine used was purchased from Sigma–Aldrich and was used as received. The applied titanium dioxide was P25 from Degussa AG (Dusseldorf, Germany).

2.2. Instrumentation

The HPLC–UV/vis–MS equipment and procedure, light sources, and photon-counting device have recently been described [18]. The heated capillary of the ion trap mass spectrometer was set to 200 °C. ^{1}H NMR was obtained using a 600-MHz INOVA spectrometer from Varian Inc. (Palo Alto, CA, USA).

2.3. Synthesis of Bu_4N^+, $[Ru(Hdcbpy)_2(NCS)(4\text{-TBP})]^-$

N719 (25 mg, 0.021 mmol) and a large excess of 4-*tert*-butylpyridine (320 μl, 2.14 mmol) were dissolved in DMF (5 ml). The solution was deaerated with argon and heated to approximately 120 °C under a small argon flow. After ∼24 h, the solvent was removed by means of rotary evaporation and the remaining solids were dissolved in a small amount of methanol. The solution was separated on a column packed with Sephadex LH20 resin and with the application of a starting eluent of water/acetonitrile/formic acid (94/5/1). Methanol was added during the elution process until all ruthenium complexes were eluted. The eluted fractions were analyzed using LC–UV/vis–MS; the fractions containing the desired substitution product were collected and the solvent was removed by means of rotary evaporation. The remaining solid product was dissolved in 1.1 g of D_2O and 40 μl of a basic solution of 1 g D_2O and 100 mg NaOD, and the solution was analyzed using ^{1}H NMR.

2.4. Preparation of a dyed TiO_2 colloidal solution

The preparation of dye-covered Degussa P25 TiO_2 particles has recently been described [18]. In brief, TiO_2 (600 mg) was magnetically stirred in 250 ml of an **N719** dye solution ([N719] = 6.1×10^{-5} mol/l) in absolute ethanol. After 24 h, the ethanol was removed by means of rotary evaporation and the dry and dyed particles were isolated. Some of the dyed nanocrystalline TiO_2 powder (12 mg dyed with 0.304 μmol **N719**) was placed into a cuvette containing 3 ml of dry acetonitrile and 230 μl of 4-*tert*-butylpyridine (1.50 mmol, [4-TBP] = 0.5 M). The mixture was degassed with a flow of argon for 20 min. After degassing, a "homogenous" stable dyed TiO_2 colloidal solution was obtained by sonification of the cuvette for 1 h.

2.5. Photolysis of N719-dyed TiO_2 particles in the presence of 4-TBP

The cuvette containing the dyed colloidal TiO_2 solution was placed in the black box of a photon-counting device. The sample was irradiated with light (532 nm) with an intensity of ~6 mW/cm^2 for 45–360 min, corresponding to a light dose of 1×10^5–10^6 counting numbers (1×10^5 counting numbers = 5.55×10^{-5} mol of photons). After the photolysis was stopped, the dyed TiO_2 colloidal solution was transferred into a round-bottomed flask, and the acetonitrile was removed by means of rotary evaporation. The degradation products were extracted from the TiO_2 surface by treatment with a solution composed of 2 ml of 0.1 M NaOH and 1 ml of ethanol. The TiO_2 particles are white after the base treatment indicating that the dye extraction is complete. The red extract was transferred into a clean test tube and centrifuged. The red supernatant was transferred into another test tube to which 15 μl of formic acid was then added. The acidified solution was transferred into an HPLC vial and analyzed using LC–UV/vis–MS. The LC–UV/vis chromatograms were recorded in the maximum absorption mode in the 400–800-nm wavelength interval. LC–MS chromatograms were extracted as the total ion chromatogram of the *m/z* values 643, 648, 675, 689, 706, and 783.

2.6. Response factor calculations

The UV/vis and MS response factors of Bu_4N^+ $[Ru(Hdcbpy)_2(NCS)(4\text{-TBP})]^-$ relative to **N719** were obtained from samples containing known concentrations of the isolated substitution products **SP** and **N719**. The following values were obtained: $(R_{SP}/R_{N719})_{UV} = 1.22$ and $(R_{SP}/R_{N719})_{MS} = 3.15$. The UV and MS response factors of **3–6** were assumed to equal the response factors of **N719**.

2.7. Photo-induced absorption spectroscopy

The photo-induced absorption (PIA) apparatus has been described elsewhere [19]. Briefly, a 1.0-mm path-length cuvette containing the dyed TiO_2 sample and 4-*tert*-butylpyridine (0, 0.5, or 1 M) was illuminated with chopped green light from a high-intensity Luxeon Star light-emitting diode (1 W, λ_{max} = 530 nm) from Lumileds Lighting, LLC (San Jose, CA, USA). The light intensity was controlled electronically in the range of 0.2–7.5 mW cm^{-2}. The resulting absorption changes at 800 nm were probed with light from a filtered tungsten-halogen lamp ($\lambda > 715$ nm) using a monochromator, an Si detector, and a lock-in amplifier set at the chopping frequency (range, 1000–1 Hz). Time constants were obtained using a non-linear, least squares fit of the frequency domain data.

3. Results and discussion

3.1. Identification of the substitution product

Fig. 2a presents an LC–MS chromatogram of an aliquot of the reaction mixture of **N719** and **4-TBP** in DMF after 9 h of heating at 120 °C.

The peak with a retention time of 9.01 min was identified as the fully protonated starting complex, $[Ru(H_2dcbpy)_2(NCS)_2]$. The complex was characterized by its visible absorption spectrum of λ_{max} = 525 nm and by a characteristic ruthenium isotope pattern around the M^+ ion, $[Ru^{(III)}(H_2dcbpy)_2(NCS)_2]^+$, *m/z* = 706 [18,21]. The peak with a retention time of 10.15 min had a maximum in the visible spectrum at λ_{max} = 509 nm and an intense ruthenium isotope pattern in the mass spectrum around the ion *m/z* = 783, which was consistent with the mass of the

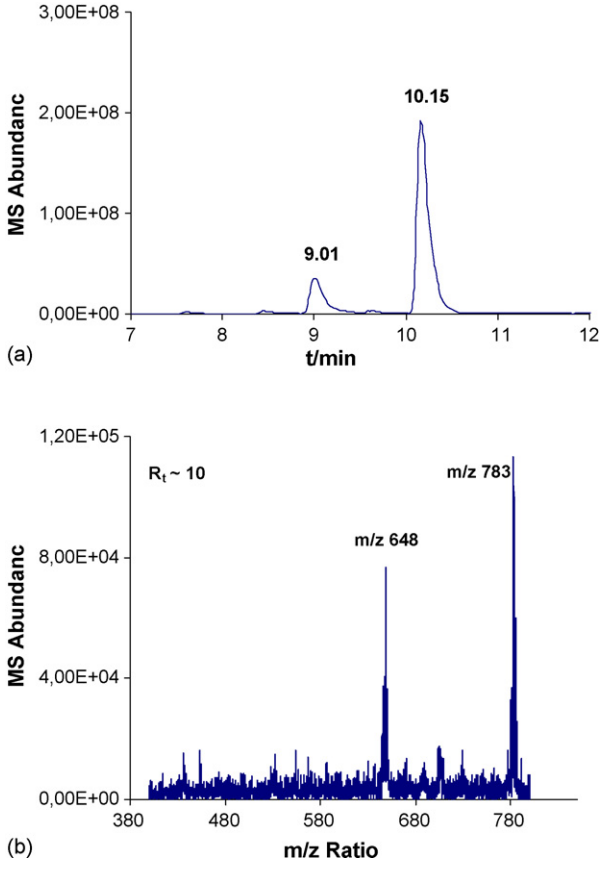

Fig. 2. (a) Total ion chromatogram of a DMF solution of **N719** (0.2 mM) and **4-TBP** (0.2 M) after 9 h heating at 120 °C; (b) mass spectrum of the peak eluting at 10.15 min.

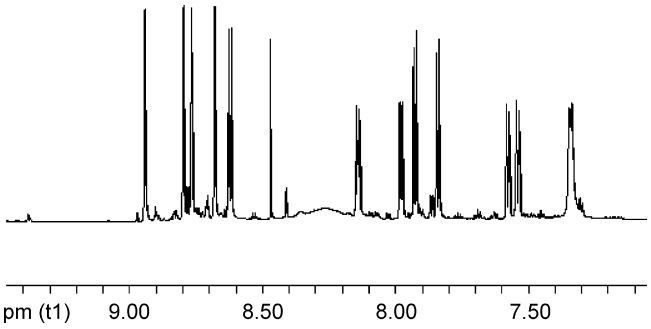

Fig. 3. ^{1}H NMR spectrum of the aromatic region of Bu_4N^+, $[Ru(Hdcbpy)_2(NCS)(4\text{-TBP})]^-$.

$[M+H]^+$ ion $[Ru^{(II)}(H_2dcbpy)(Hdcbpy)(NCS)(4\text{-TBP})+H]^+$ (see Fig. 2b). The fragment ion $m/z = 648$ corresponds to the ion $[Ru^{(II)}(H_2dcbpy)_2(NCS)]^+$ formed by elimination of the **4-TBP** ligand from the molecular ion.

To confirm the structure using ^{1}H NMR, the reaction was performed at a larger scale followed by purification of the **4-TBP**-substituted complex on a sephadex column using an eluent mixture of water, acetonitrile, and formic acid. The ^{1}H NMR spectrum of the purified product shows 14 non-equivalent aromatic protons (Fig. 3) and a singlet at 1.5 ppm. The molecule has 12 aromatic bipyridine signals, which indicate a complex with the structure $[Ru(H_2dcbpy)_2XY]$, in which the two bipyridyl groups are non equivalent. The four H3 and H3′ protons of the two bipyridyl rings can be identified from their small doublet splitting, $^4J \approx 1$ Hz, and the eight H5, H6, H5′, and H6′ protons by their doublet splitting, $^3J = 6$–7 Hz. The last two aromatic signals at 7.34 and 7.33 ppm are due to the four aromatic protons on the pyridine ring, while the signal at 1.5 ppm is due to the *tert*-butyl group. The MS and ^{1}H NMR spectra are therefore consistent with the structure depicted in Fig. 1, in which X = NCS and Y = 4-TBP.

3.2. $TiO_2 \mid S^+ + 4\text{-}TBP + light$

Fig. 4 presents a typical LC–MS chromatogram of a dye extract obtained from a model experiment, in which a colloidal solution of **N719**-dyed nanocrystalline TiO_2 particles in acetonitrile-containing **4-TBP** (0.5 M) have been irradiated with 532-nm laser light at an intensity of $I_0 = 6.2$ mW/cm^2. Six peaks are observed in the LC–MS chromatogram. The two peaks at $R_t = 9.4$ and 8.9 min are due to the fully protonated starting complex, $[Ru(H_2dcbpy)_2(NCS)_2]$, and its minor isomer, $[Ru(H_2dcbpy)_2(NCS)(SCN)]$, respectively. The peak at $R_t = 10.3$ min is identified as the 4-*tert*-butylpyridine substitution product, **SP**, whereas the peaks at $R_t = 4.9$, 6.4, 6.9, and 7.3 min are identified as the fully protonated **N719** degradation products **6**, **5**, **4**, and **3**, respectively. No trace of the disubstituted complex $[Ru(Hdcbpy)_2(4\text{-TBP})_2]$ was detected. This is likely due to the fact that the visible spectrum of the precursor mono substituted complex **SP** is blue shifted (16 nm) relative to **N719** which means that very few **SP** molecules are excited at 532 nm.

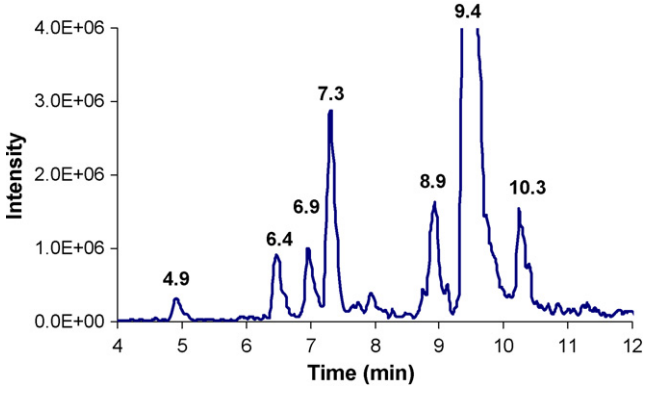

Fig. 4. LC–MS chromatogram of the dye extract obtained after photolysis ($\lambda = 532$ nm) of ~12 mg of colloidal solution of **N719**-dyed nanocrystalline TiO_2 particles containing **4-TBP** (0.5 M) in acetonitrile. Applied light intensity $I_0 = 6.3$ mW/cm^2 and light dose = 2.7×10^{-4} mol photons.

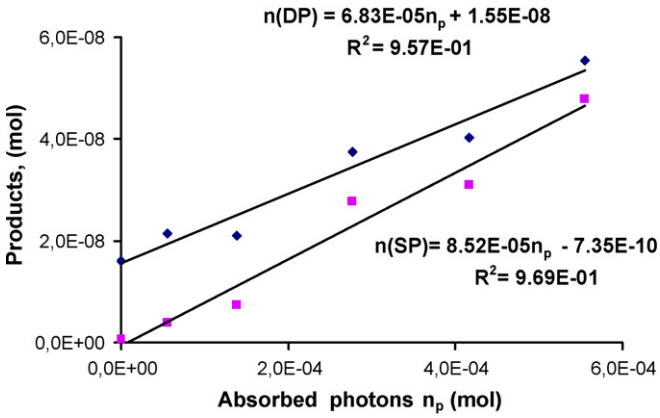

Fig. 5. Amount of substitution products, **SP** (■), and the sum of degradation products (DP) **3–6** (♦), of the photolysis experiments as a function of light dose [4-TBP] = 0.5 M.

The λ_{max} and the characteristic m/z values of the identified products are shown in Table 1.

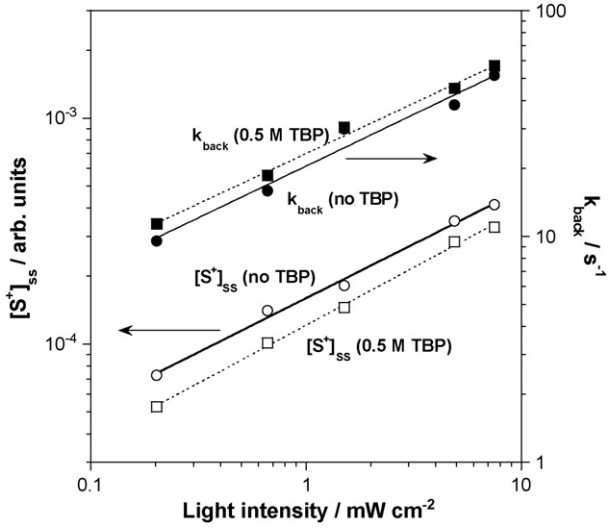

Fig. 6. Light intensity dependence of the steady-state concentration of oxidized dye, $[S^+]_{ss}$, and the recombination rate constant, k_{back}, obtained by means of photo-induced absorption (PIA) spectroscopy. Lines correspond to power-law fits.

Table 1
Identified products obtained from the 532-nm laser light photolysis of N719-dyed nanocrystalline TiO_2 particles in acetonitrile, containing **4-TBP** (0.50 M)

Compound (M)[a]	R_t (min)	λ_{max} (nm)	m/z[b]	Mol × 10^8
$[Ru(H_2dcbpy)_2(NCS)(NCS)]$	9.4	525	706 $[M]^+$[c,d]	21.4
$[Ru(H_2dcbpy)_2(NCS)(SCN)]$	8.8	521	706 $[M]^+$	2.5
$[Ru(H_2dcbpy)(Hdcbpy)(NCS)(4\text{-}TBP)]$	10.3	509	783 $[M+H]^+$	1.6
$[Ru(H_2dcbpy)(Hdcbpy)(NCS)(CH_3CN)]$	7.3	490	689 $[M+H]^+$	3.4
$[Ru(H_2dcbpy)_2(NCS)(CN)]$	6.9	497	675 $[M+H]^+$	1.1
$[Ru(H_2dcbpy)(Hdcbpy)(NCS)(H_2O)]$	6.4	497	688 $[M+Na]^+$[e]	1.1
$[Ru(H_2dcbpy)_2(CN)_2]$	4.9	473	643 $[M+H]^+$	0.4

The laser intensity was 6.3 mW/cm^2 and the number of absorbed photons was 2.7×10^{-4} mol.
[a] We have assumed that M are eluted as neutral complexes through the RP C18 HPLC column.
[b] The reported m/z values correspond to the most intense signals in the observed ruthenium isotope clusters.
[c] The assignment of the m/z values is based on the ^{102}Ru isotope.
[d] The fragmentation ion $m/z = 648$ is observed in all the mass spectra except for $[Ru(H_2dcbpy)_2(CN)_2]$.
[e] A minor ruthenium isotope cluster around $m/z = 666$ $[M+H]^+$ is observed in the mass spectrum of the water complex.

Table 2
Relationships between $[S^+]_{ss}$ and k_{back} as a function of I_0 and [4-TBP]

	[4-TBP] (M)	I_0 power-law[a] fits	R^2
$[S^+]$ss	0	$1.60 \times 10^{-4} \times I_0^{0.48}$	0.996
$[S^+]$ss	0.5	$1.21 \times 10^{-4} \times I_0^{0.51}$	0.995
k_{back}	0	$20.5 \times I_0^{0.46}$ s^{-1}	0.963
k_{back}	0.5	$23.3 \times I_0^{0.44}$ s^{-1}	0.993

[a] Unit of I_0 = mW/cm^2.

A series of photolysis experiments (series 3, Table 2) was performed using nearly constant laser light intensity, $I_0 = 6.2$ mW/cm^2, [4-TBP] = 0.5 M, and increasing light doses; the results are presented in Fig. 5. The quantum yield of the substitution product, Φ_{SP}, was 0.85×10^{-4} and the quantum yield of the sum of the degradation products **3–6**, Φ_{DP}, was 0.68×10^{-4}; these values may be obtained as the slopes of the straight lines depicted in Fig. 5. The intercept of the DP line with the y-axis (see Fig. 5) is due to an initial formation of the DP product $[Ru(H_2dcbpy)_2(NCS)(CN)]$ before the start of photolysis. The origin of this initial product formation is unknown; however, impurity defects in the Degussa P25 nanoparticles may be responsible for the formation of $TiO_2 \mid S^+$ followed by the formation of $[Ru(H_2dcbpy)_2(NCS)(CN)]$.

3.3. Determination of K_{back}

To investigate the effect of **4-TBP** on the back electron-transfer rate, k_{back}, PIA measurements were performed on colloidal mixtures of **N719**-sensitized TiO_2 particles in acetonitrile in the presence of 0 or 0.5 M **4-TBP**. The absorption of the oxidized form of **N719** was monitored at 800 nm at various excitation intensities. From the frequency dependence of the PIA response, the (pseudo-) first-order rate constant, k_{back}, and the steady-state concentration of S^+ were derived. The equations describing the correlation curve of $[S^+]_{ss}$ and k_{back} at intensity I_0 with either 0 or 0.5 mol/l of **4-TBP** are presented as formulas in Table 2 and depicted graphically in Fig. 6.[1]

Both k_{back} and $[S^+]_{ss}$ increase, according to a power law, with excitation light intensity. The exponent is close to 0.5 for all curves. This suggests that the recombination of oxidized dye molecules with electrons in the TiO_2 particles follows second-order kinetics. The addition of 0.5 M **4-TBP** leads to a significant decrease in the steady-state concentration of S^+, while k_{back} is less affected. The back electron-reaction rate under steady-state conditions, given by $v_{back} = k_{back} \times [S^+]_{ss}$, appears to be slightly reduced upon addition of 0.5 M **4-TBP**, which suggests that the electron injection rate from excited dye into the TiO_2 is slightly reduced. Such a decrease in injection efficiency is consistent with a general trend towards slightly reduced photocurrents upon the addition of **4-TBP** to the electrolyte [20].

3.4. Mechanism of substitution

A series of photolysis experiments were performed in which the **4-TBP** concentrations were varied from 0 to 1 M while the light intensity was kept constant (≈6.8 mW/cm^2). From Fig. 7 it is evident that the quantum yield of substitution product **SP**, Φ_{SP}, increases as a function of [4-TBP], whereas the sum of the quantum yields of the degradation products **3–6**, Φ_{DP}, decrease. As seen in Table 3, the sum of quantum yields of all five degradation products, $\Phi_{deg} = \Phi_{DP} + \Phi_{SP}$, is nearly constant, independent of the additive concentration. If the $[Ru^{III}(H_2dcbpy)_2(NCS)]^+$ complex was substituted directly by **4-TBP**, then Φ_{DP} would be independent of the **4-TBP** concentration, as long as $k_{back} \gg k_{deg}$;

[1] In previous work [18] we measured back electron-transfer rates in absence of **4-TBP** that were approximately four times higher ($k_{back} = 78.7 I_0^{(0.404)}$ s^{-1}) than in current work. The PIA experiments were performed on dyed TiO_2 particles prepared according to method I in Ref. [18]. In this procedure, TiO_2 particles were sprayed onto a glass plate and sintered at 450 °C, after which the glass plate was soaked in a solution of **N719**. The dyed TiO_2 particles were then scraped off the glass plate and used to prepare a colloidal solution in acetonitrile. Careful repeated PIA experiments gave reproducible k_{back} values and did not reveal any significant differences in the back electron transfer rates obtained by the current TiO_2 sample preparation method and the method I in Ref. [18]. In the first series of measurements [18] we used a chopped green laser, whereas in the present work an on/off modulated light emitting diode (530 nm) was applied. A possible explanation of the four-fold divergence between our previously published k_{back} values and those presented in this work might be due to the differences in the uniformity of the excitation light, which is much better in this work. We do not, however, have evidence for this speculative explanation.

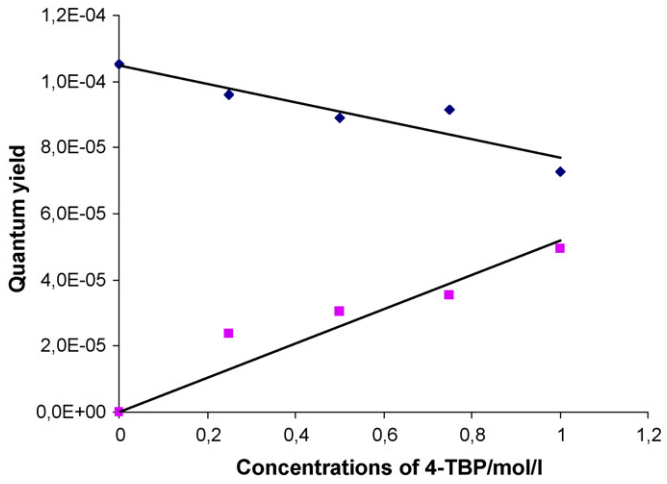

Fig. 7. Quantum yields, Φ_{SP}, of the substitution product, **SP** (■), and quantum yields, Φ_{DP}, of the sum of degradation products **3–6** (♦), as a function of the concentration of **4-TBP**.

Φ_{deg} would therefore increase as a function of [4-TBP]. The quantum yield data therefore indicate that the Ru^{III} complex is not substituted directly by **4-TBP**. This is in line with the generally accepted understanding that the ligands of Ru^{III} complexes are generally more strongly bonded to the metal center than is the case in the corresponding Ru^{II} complexes [22]. At room temperature, the $[Ru^{II}(H_2dcbpy)_2(NCS)_2]$ complex is very stable towards the **4-TBP** substitution reaction, so the $[Ru^{III}(H_2dcbpy)_2(NCS)_2]^+$ complex should therefore react even slower with nucleophiles.

An alternative mechanism is proposed in Fig. 8, in which both the substitution and degradation products **3–6** are formed through a common intermediate. The reaction is initiated by an internal electron-transfer reaction between the thiocyanate ligand and the Ru^{III} center in **N719**, with the formation of an intermediate complex, $[Ru^{II}(H_2dcbpy)_2(NCS)(NCS\cdot)]$ [18,23]. This intermediate complex, **I**, may subsequently react with the solvent (CH_3CN), the additive **4-TBP**, trace of water or degrade to form the $[Ru(H_2dcbpy)_2(NCS)(CN)]$ complex. If the solvent is changed to dimethylformamide no solvent derived product $[Ru(H_2dcbpy)(Hdcbpy)(NCS)(DMF)]$ is obtained indicating that DMF is reacting much slower than CH_3CN with the complex I.

According to the mechanism depicted in Fig. 8, the rate of degradation of $TiO_2 \mid S^+$ is exclusively determined by the rate of the internal electron transfer between the ligand, NCS^-, and the Ru^{III} metal center, k_{deg}, and does not depend on the **4-TBP** concentration. The amounts of **SP** and **DP** products **3–6**, however, will increase and decrease, respectively, with increasing **4-TBP** concentration, in reasonable agreement with the experimental results.

3.5. Calculation of k_{deg}

An expression for the rate of degradation, k_{deg} (Eq. (8)), may be derived by applying the steady-state approximation to Eqs. (1), (2), (6), and (7) and using the relationship $k_{back} \gg k_{deg}$:

$$TiO_2|S^+ \xrightarrow{k_{deg}} TiO_2|\text{intermediate} \xrightarrow{\text{4-TBP}} TiO_2|SP + TiO_2|DP \quad (7)$$

$$k_{deg} \approx f_c \times \Phi_{deg} \times k_{back}, \qquad f_c = 0.60,$$
$$\Phi_{deg} = \Phi_{DP} + \Phi_{SP}, \qquad \Phi_{DP} = \Phi_3 + \Phi_4 + \Phi_5 + \Phi_6 \quad (8)$$

The correction factor, f_c, in Eq. (8) compensates for the fact that the light intensity decreases from its initial value, I_0, at the entrance of the photolysis cuvette, to a very small value after passing through the 1 cm dyed TiO_2 colloidal solution. This will cause the back electron-transfer rate to decrease throughout the cell [18]. The calculated k_{deg} values are presented in Table 3. It is seen that the degradation rates are reasonably constant, independent of the applied **4-TBP** concentration, as predicted by the mechanism presented in Fig. 8. The average degradation rate was found to be $\langle k_{deg} \rangle = (4.1 \pm 0.5) \times 10^{-3}\ s^{-1}$. We have previously published a value that was 10 times greater, i.e., $k_{deg} = 4 \times 10^{-2}\ s^{-1}$ [18]. This value was based on k_{back} rates that were approximately four times faster than the k_{back} rates presented here. The PIA measurements were repeated several times, producing, each time, the same results as shown in

Table 3
Quantum yields[a] of degradation as a function of light intensity and [4-TBP]

Exp. series	[4-TBP] M	I (mW/cm^2)	k_{back} (s^{-1})	$\Phi_{DP} \times 10^4$	$\Phi_{SP} \times 10^4$	$\Phi_{deg} \times 10^4$	$k_{deg} \times 10^3\ s^{-1}$
1	0	6.2	47	1.1	0	1.2	3.4
2	0	8.2	47	1.6	0	1.6	4.5
3	0.5	6.2	53	0.68	0.85	1.5	4.8
4	0.5	6.2	53	0.71	0.66	1.4	3.4
5	0.5	5.2	53	0.82	0.77	1.5	4.8
6	0.7	13.0	79	0.36	0.61	1.0	4.7
7	0	6.2	47	1.1	0	1.1	3.1
8	0.25	6.7	53	0.96	0.24	1.2	3.8
9	0.50	7.6	53	0.89	0.30	1.2	3.8
10	0.75	6.7	53	0.91	0.35	1.3	4.1
11	1.00	6.8	53	0.73	0.49	1.2	3.8
Average						1.3 ± 0.2	4.1 ± 0.5
Nour-Mohammadi, et al. [18]							7.5 ± 1.0

[a] $\Phi_{deg} = \Phi_{DP} + \Phi_{SP}$; $\Phi_{DP} = \Phi_3 + \Phi_4 + \Phi_5 + \Phi_6$.

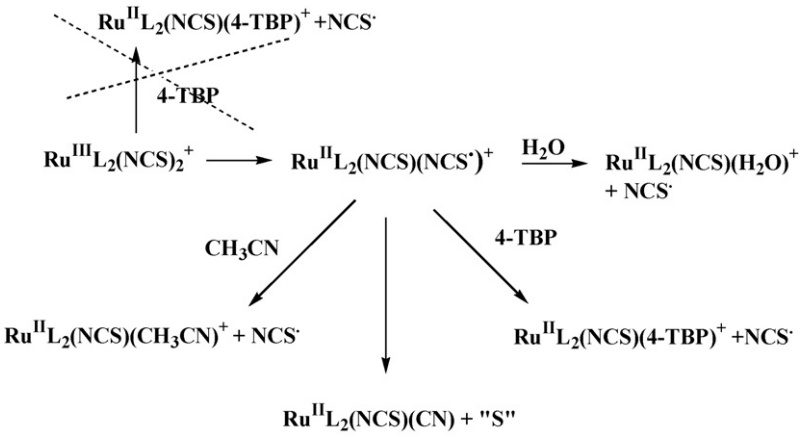

Fig. 8. Degradation mechanism of $TiO_2 \mid RuL_2(NCS)_2^+$, where $L = H_2$dcbpy. The bonds between the ruthenium complexes and the TiO_2 surface are not shown in the figure.

Table 2. We therefore believe that the k_{back} values obtained in this work are more reliable than those previously presented. Applying the k_{back} values obtained in this work (see Table 2), and slightly adjusting our old actinometry data, reduces our previously published degradation rate by a factor of ~5, to $k_{deg} = 7.5 \times 10^{-3}\ s^{-1}$. We have no good explanation of this two-fold divergence between our old and new degradation values. The average degradation rate is $k_{deg} = 6 \times 10^{-3}\ s^{-1}$, corresponding to a half-life of $TiO_2 \mid S^+$ (S = **N719**) of greater than 100 s. In contrast, the lifetime of $[Ru^{III}(H_2dcbpy)_2(NCS)_2]^+$ in homogenous solution is in the ms range, judging from the irreversible cyclic voltammograms of **N3** and **N719** [23]. Apparently, the oxidized form of the dye is stabilized when it is attached to the TiO_2 surface. The surface stabilization has recently been suggested to be due to the formation of a $O_2Ti^{(III)}$–O–C(O)–L–$Ru^{(III)}(H_2dcbpy)_2(NCS)_2$ complex after the initial electron injection [24a, b]. In this complex back bonding interaction with transfer of electron density from Ti(III) to the ligand π^* orbitals should stabilize the ruthenium (III) complex. The increase of $TiO_2 \mid S^+$ stability by a factor of 10^5 relative to S^+ in solution is certainly a key reason for the stability of **N719** during solar cell operation.

3.6. Evaluation of the lifetime of the N719 dye in solar cells with 4-TBP addition

The evaluation of **N719** dye stability is based on a simple lifetime estimation in which it is assumed that the $TiO_2 \mid S^+$ reaction (Eq. (7)) is the only side reaction in the solar cell, and that the kinetics of the simple model system are similar to the degradation kinetics of a real solar cell [18]. The lifetime calculation of the sensitizer is based on the prediction of the turnover number, *N*, i.e., the number of cell cycles that a single sensitizer molecule should be able to sustain. *N* can be estimated using the following simple expression (Eq. (9)), where k_{reg} is the rate of electron transfer between iodide and $TiO_2 \mid S^+$:

$$N = k_{reg} \times \frac{[I^-]}{k_{deg}} \tag{9}$$

It has previously been estimated that the sensitizer should be able to sustain 1×10^8 cell cycles in order to obtain a dye lifetime of 20 y of normal solar cell operation [4]. The estimated value of *N* may therefore be converted into sensitizer lifetime using Eq. (10):

$$\text{lifetime of } S = 20 \text{ years} \times \frac{N}{1 \times 10^8} \tag{10}$$

The regeneration rates, k_{reg}, of **N3** (the fully protonated form of **N719**) attached to the nanocrystalline TiO_2 have been obtained by several groups by means of laser flash photolysis experiments [25,26]. The regeneration rates range between $k_{reg} = 2.1 \times 10^5\ M^{-1}\ s^{-1}$ [26a,b] and $4.3 \times 10^7\ M^{-1}\ s^{-1}$ [25a,c]. The reason for such large divergences between these experimentally obtained regeneration values is not obvious; however, k_{reg} is apparently highly dependent on particular experimental conditions. Based on an average value $k_{reg} = 2 \times 10^6\ M^{-1}\ s^{-1}$ for **N3** and the average degradation rate, $k_{deg} = 6 \times 10^{-3}\ s^{-1}$, a turnover number, *N*, of 1.7×10^8 may be calculated using Eq. (9) (see Table 4). This number corresponds to ~34 years of normal solar cell operation indicating that the **N719** sensitizer is perfectly stable under normal solar cell operation at room temperature.

In the introduction it was mentioned that the substitution product **SP** was detected in light-exposed DSSC solar cells. Substantially amounts of **SP** and **3–6** were observed after only 5 weeks of continuous irradiation with 800 W/m^2 simulated sunlight [16]. This finding is apparently in contradiction with the

Table 4
Lifetime estimates of **N719** dye under normal solar cell operation using $K_{deg} = 6 \times 10^{-3}\ s^{-1}$ [a]

k_{reg} ($M^{-1}\ s^{-1}$) [a]	Turnover number (*N*)	Dye lifetime (years)
2.1×10^5 [b]	1.8×10^7	4
2×10^6 [c]	1.7×10^8	34
4.3×10^7 [d]	2.9×10^9	750

[a] Average value of the degradation values obtained in this work and in Nour-Mohammadi, et al. [18].
[b] Ref. [26a].
[c] Average regeneration value.
[d] Ref. [25a].

predicted long-term stability of **N719**. The observed dye degradation, however, was most likely caused by loss of solvent and electrolyte due to imperfect sealing of the cells.

4. Conclusions

The substitution product Bu_4N^+, $[Ru(Hdcbpy)_2(NCS)(4\text{-}TBP)]^-$ may be synthesized in a simple homogeneous thermal reaction in DMF between the solar cell dye **N719** and the additive **4-TBP**. The same product is formed by the photolysis of a colloidal solution of **N719**-dyed TiO_2 particles in the presence of **4-TBP**. At constant illumination intensity, the total quantum yield, Φ_{deg}, of the five degradation products, i.e., $[Ru(H_2dcbpy)(Hdcbpy)(NCS)(4\text{-}TBP)]$, $[Ru(H_2dcbpy)_2(NCS)(CN)]$, $[Ru(H_2dcbpy)(Hdcbpy)(NCS)(CH_3CN)]$, $[Ru(H_2dcbpy)(Hdcbpy)(NCS)(H_2O)]$, and $[Ru(H_2dcbpy)_2(CN)_2]$, is constant, indicating that these products are formed through a common intermediate. We suggest that the structure of the intermediate is $[Ru^{II}(H_2dcbpy)_2(NCS)(NCS\cdot)]^+$, which may be generated via a rate-determining internal electron-transfer rate, k_{deg}, between the thiocyanate ligand and the Ru^{III} metal center in the **N719** dye. The k_{deg} values obtained in this and in our previous study [18] are $4–8 \times 10^{-3}\ s^{-1}$. The k_{deg} values are independent of **4-TBP** addition at room temperature, so **4-TBP** does not decrease the lifetime of the solar cell. Based on the average k_{deg} value of $6 \times 10^{-3}\ s^{-1}$ and an average regeneration reaction between $TiO_2 \mid S^+$ and iodide $k_{reg} = 2 \times 10^6\ M^{-1}\ s^{-1}$, a lifetime of ~34 years is predicted for the **N719** sensitizer under normal solar cell operation indicating no stability problems with **N719** due to **4-TBP** addition. The **N719** dye may, however, react with **4-TBP** in the solar cell by a thermal substitution reaction at elevated temperatures. Such a thermal reaction is likely to decrease the lifetime of the dye.

References

[1] B. O'Regan, M. Grätzel, Nature 353 (1991) 737.
[2] A. Hagfeldt, M. Grätzel, Chem. Rev. 95 (1995) 49.
[3] M. Grätzel, Coord. Chem. Rev. 77 (1998) 347.
[4] M. Grätzel, A. Hagfeldt, Accounts Chem. Res. 33 (2000) 269.
[5] N. Vlachopoulos, L. Liska, J. Augusrynski, M. Grätzel, J. Am. Chem. Soc. 110 (1988) 1216.
[6] M.K. Nazeeruddin, A. Kay, I. Rodicio, R. Humphry-Baker, E. Miiller, P. Liska, N. Vlachopoulos, M. Grätzel, J. Am. Chem. Soc. 115 (1993) 6382.
[7] H. Kusama, H. Arakawa, J. Photochem. Photobiol. A: Chem. 160 (2003) 171.
[8] H. Kusama, K. Konishi, H. Sugihara, H. Arakawa, Sol. Energy Mater. Sol. Cells 80 (2003) 167.
[9] H. Kusama, H. Arakawa, Sol. Energy Mater. Sol. Cells 81 (2004) 87.
[10] H. Kusama, H. Arakawa, J. Photochem. Photobiol. A: Chem. 162 (2004) 441.
[11] H. Kusama, H. Arakawa, Sol. Energy Mater. Sol. Cells 82 (2004) 457.
[12] O. Kohle, M. Gratzel, A.F. Meyer, T.B. Meyer, Adv. Mater. 9 (1997) 904.
[13] G. Schlichthorl, S.Y. Huang, J. Sprague, A.J. Frank, J. Phys. Chem. B 101 (1997) 8139.
[14] G. Boschloo, L. Haggman, A. Hägfeldt, J. Phys. Chem. B 110 (2006) 13144.
[15] S.Y. Huang, G. Schlichtörl, A.J. Nozik, M. Grätzel, A.J. Frank, J. Phys. Chem. B 101 (1997) 2576.
[16] T. Lund, et al., in preparation.
[17] G. Benkö, P. Myllyperkiö, J. Pan, A.P. Yartsev, V. Sundström, J. Am. Chem. Soc. 125 (2003) 1118–1119.
[18] F. Nour-Mohammadi, S.D. Nguyen, G. Boschloo, A. Hagfeldt, T. Lund, J. Phys. Chem. B 109 (2005) 22413.
[19] G. Boschloo, A. Hagfeldt, Chem. Phys. Lett. 370 (2003) 381.
[20] G. Boschloo, H. Lindstrom, E. Magnusson, A. Holmberg, A. Hagfeldt, J. Photochem. Photobiol. A: Chem. 148 (2002) 11–15.
[21] G. Hansen, B. Gervang, T. Lund, Inorg. Chem. 42 (2003) 5545.
[22] L. Helm, A. Merbach, Chem. Rev. 105 (2005) 1923–1959.
[23] F. Cecchet, A.M. Gioacchini, M. Marcaccio, F. Paolucci, S. Roffia, M. Alebbi, C.A. Bignozzi, J. Phys. Chem. B 106 (2002) 3926.
[24] (a) H. Tributsch, Coord. Chem. Rev. 248 (2004) 1511–1530;
(b) Th. Dittrich, B. Neumann, H. Tributsch, J. Phys. Chem., submitted for publication.
[25] (a) S.A. Haque, Y. Tachibana, D.R. Klug, J.R. Durrant, J. Phys. Chem. B 102 (1998) 745;
(b) S. Pelet, J.E. Moser, M. Gratzel, J. Phys. Chem. B. 104 (2000) 1791;
(c) T.A. Heimer, E.J. Heilweil, C.A. Bignozzi, G.J. Meyer, J. Phys. Chem. A: Mol. Spectrosc. Kinet. Environ. Gen. Theory 104 (2000) 4256.
[26] (a) D. Kuciauskas, M.S. Freund, H.B. Gray, J.R. Winkler, N.S. Lewis, J. Phys. Chem. B 105 (2001) 392;
(b) I. Montanari, J. Nelson, J.R. Durrant, J. Phys. Chem. B 106 (2002) 12203.